TE and TM guided modes in an air waveguide with negative-index-material cladding

G. D'Aguanno,[1,2,*] N. Mattiucci,[1,2,3] M. Scalora,[2] and M. J. Bloemer[2]
[1]*Time Domain Corporation, Cummings Research Park 7057 Old Madison Pike Huntsville, Alabama 35806, USA*
[2]*Research Development and Engineering Center, U.S. Army Aviation & Missile Command, Building 7804, Redstone Arsenal, Alabama 35898-5000, USA*
[3]*Università "RomaTre," Dipartimento di Fisica "E. Amaldi," Via Della Vasca Navale 84, I-00146 Rome, Italy*
(Received 4 November 2004; revised manuscript received 6 December 2004; published 5 April 2005)

We numerically demonstrate that a planar waveguide in which the inner layer is a gas with refractive index $n_0=1$, sandwiched between two identical semi-infinite layers of a negative index material, can support both transverse electric and transverse magnetic guided modes with low losses. Recent developments in the design of metamaterials with an effective negative index suggest that this waveguide could operate in the infrared region of the spectrum.

DOI: 10.1103/PhysRevE.71.046603 PACS number(s): 41.20.Jb

I. INTRODUCTION

Negative-index materials (NIMs)—i.e., materials that have simultaneously negative electric susceptibility and magnetic permeability—seem to challenge several well-established concepts in electromagnetism and optics. Perhaps the best known examples are their ability to refract light in the opposite way with respect to what an ordinary material does [1] and the possibility to use them to construct a "perfect" lens—i.e., a lens that can focus all Fourier components of a two-dimensional (2D) image, even those that do not propagate in a radiative manner [2]. One of the first experimental demonstrations of negative-index behavior was accomplished by Shelby *et al.* in 2001 [3], who showed negative refraction of microwaves in a material made by a two-dimensional array of repeated unit cells of copper strips and split-ring resonators. A large number of papers have been published on the subject just in the last few years and a review can be found in Ref. [4].

In optics it is well known that when the inner layer of a planar waveguide is a gas with refractive index $n_0=1$ and it is sandwiched by two standard dielectric materials with refractive index $n>1$, total internal reflections cannot be achieved. The field coupled inside such a waveguide attenuates in the propagation direction by leaking power to the two bounding media [5]. The losses suffered via these "leaky" modes may be balanced when the molecular gas in the core is an active medium, as, for example, in CO_2 waveguide lasers [6,7]. In metal-clad waveguides [8] the refractive index of the guiding layer can be arbitrarily low as long as it is greater than the refractive index of the substrate. Total internal reflections are always achieved thanks to the low refractive index of the metal. In Ref. [8] guiding has been demonstrated in an air-polystyrene-silver waveguide at optical frequencies, in a 1.81-μm-thick polystyrene film. Losses were estimated at approximately 1 dB/cm for the fundamental TE mode. The theory of hollow waveguides has been developed in Ref. [9], and different types of hollow waveguides in the infrared have been realized during the years. We cite, for example, hollow sapphire fibers [10], hollow Ag/AgI-coated glass waveguides [11], and ZnS-coated Ag hollow waveguides [12]. These guides have losses as low as 0.1 dB/m at 10.6 μm, for a bore diameter of approximately 1000 μm. In the visible region, a tremendous breakthrough in the possibility of confining light in air was achieved at the end of 1999, with the introduction of so-called photonic crystal fibers (PCFs) [13,14]. In a PCF light confinement does not require a core with a higher refractive index because guidance is achieved not by total internal reflection, but by the presence of a cladding in the form of a full two-dimensional photonic band gap. We note also that PCFs are single-mode fibers, while traditional hollow waveguides are highly multimodal. On the other hand, the fundamental mode in traditional hollow waveguides has generally a much longer attenuation length than all higher-order modes thanks to lower diffraction losses. Therefore, it is clear that for some applications the initial presence of many modes can be easily overcome.

The aim of this work is to demonstrate that light can be confined in air also by using a waveguide where the bounding medium, or cladding, is made of a NIM. In this case the confinement is due, as in classical waveguides, to total internal reflections. The guiding properties of a waveguide with a core made of a NIM and a cladding composed of a standard dielectric material have been studied in Ref. [15], where it was demonstrated that guided modes are admitted. In our work we study the opposite configuration—i.e., a symmetric waveguide where an air core is surrounded by a NIM. We note that, to our knowledge, at the present time an experimental realization of a metamaterials that possess an effective negative index has been achieved only in the microwave regime [3]. In this regard, several efforts are currently underway to design NIMs at higher frequency than the microwave regime. In Refs. [16,17], for example, O'Brian and Pendry have designed a NIM in the infrared region, and its nonlinear properties also have been numerically studied. The structure consists of a periodic nanostructured array of modified split-ring resonators, which is magnetically active in the near-infrared region of the spectrum. The structure is numerically

*Corresponding author. FAX: +1-256-955-7216. Electronic address: giuseppe.daguanno@timedomain.com

demonstrated to possess a negative effective permeability at telecommunications wavelengths—i.e., 1.5 μm. Although further material development is still clearly needed, the practical realization of metamaterials in the infrared region seems to be within reach [18], and the results reported in Refs. [16–18] help to put our present work in its proper perspective.

II. BASIC EQUATIONS

Let us begin with some general considerations about the refractive index and the extinction coefficient in passive materials. The refractive index n and the extinction coefficient β of a material are found by solving the following complex, algebraic equation:

$$\hat{n}^2 = \varepsilon\mu, \tag{1}$$

where $\hat{n}=n+i\beta$ is the complex refractive index and ε and μ are the frequency-dependent, complex, electric susceptibility, and magnetic permeability functions of the medium, respectively. In general, in the case of a passive medium the law of increase of entropy determines that $\mathrm{Im}(\varepsilon)$ and $\mathrm{Im}(\mu)$, which are linked to the electric and magnetic losses respectively, *are always positive*. Moreover, to the extent that every nonsteady process is thermodynamically irreversible, $\mathrm{Im}(\varepsilon)$ *and* $\mathrm{Im}(\mu)$ *are not exactly zero for any frequency other than zero* [19].

These considerations lead to the condition that the damping term β *must be always positive* for a wave propagating in the positive direction and also that β *is never exactly zero*. Physically, this means that, slight as it may be, there is always some damping of the electromagnetic wave during its propagation. Now, by equating the real and imaginary parts of the right- and left-hand sides of Eq. (1) and by solving the corresponding system of algebraic equations with the condition $\beta>0$, we find the expressions for the refractive index and the extinction coefficient as follows:

$$n = \frac{\mathrm{Im}(\varepsilon\mu)}{\sqrt{2}\sqrt{-\mathrm{Re}(\varepsilon\mu) + \sqrt{[\mathrm{Re}(\varepsilon\mu)]^2 + [\mathrm{Im}(\varepsilon\mu)]^2}}}, \tag{2a}$$

$$\beta = \frac{\sqrt{-\mathrm{Re}(\varepsilon\mu) + \sqrt{[\mathrm{Re}(\varepsilon\mu)]^2 + [\mathrm{Im}(\varepsilon\mu)]^2}}}{\sqrt{2}}. \tag{2b}$$

We note that Eqs. (2) are valid in general for any kind of passive medium and that the sign of n depends on the sign of the quantity $\mathrm{Im}(\varepsilon\mu)$ [20].

Let us describe the electric susceptibility and the magnetic permeability of the NIM with a lossy Drude model [2,21]:

$$\varepsilon(\tilde{\omega}) = 1 - \frac{1}{\tilde{\omega}(\tilde{\omega} + i\tilde{\gamma}_e)}, \quad \mu(\tilde{\omega}) = 1 - \frac{(\omega_{pm}/\omega_{pe})^2}{\tilde{\omega}(\tilde{\omega} + i\tilde{\gamma}_m)}, \tag{3}$$

where $\tilde{\omega}=\omega/\omega_{pe}$ is the normalized frequency, ω_{pe} and ω_{pm} are the respective electric and magnetic plasma frequencies, and $\tilde{\gamma}_e=\gamma_e/\omega_{pe}$ and $\tilde{\gamma}_m=\gamma_m/\omega_{pe}$ are the respective electric and magnetic loss terms normalized with respect to the electric plasma frequency. In Fig. 1(a) we show the refractive index, the extinction coefficient, the real part of the electric susceptibility, and the real part of the magnetic permeability for a NIM whose dispersion is described by Eqs. (3). In Fig. 1(a) we have taken the following parameters: $\omega_{pm}/\omega_{pe}=0.8$ and $\tilde{\gamma}_e\approx\tilde{\gamma}_m\approx10^{-4}$. As one may expect, in the region where $\mathrm{Re}(\varepsilon)$ and $\mathrm{Re}(\mu)$ have opposite signs no propagating modes are allowed in the linear regime. The NIM becomes opaque with the complex refractive index that becomes almost a pure imaginary number, $\hat{n}\cong i\beta$, and the potential barrier is insurmountable.

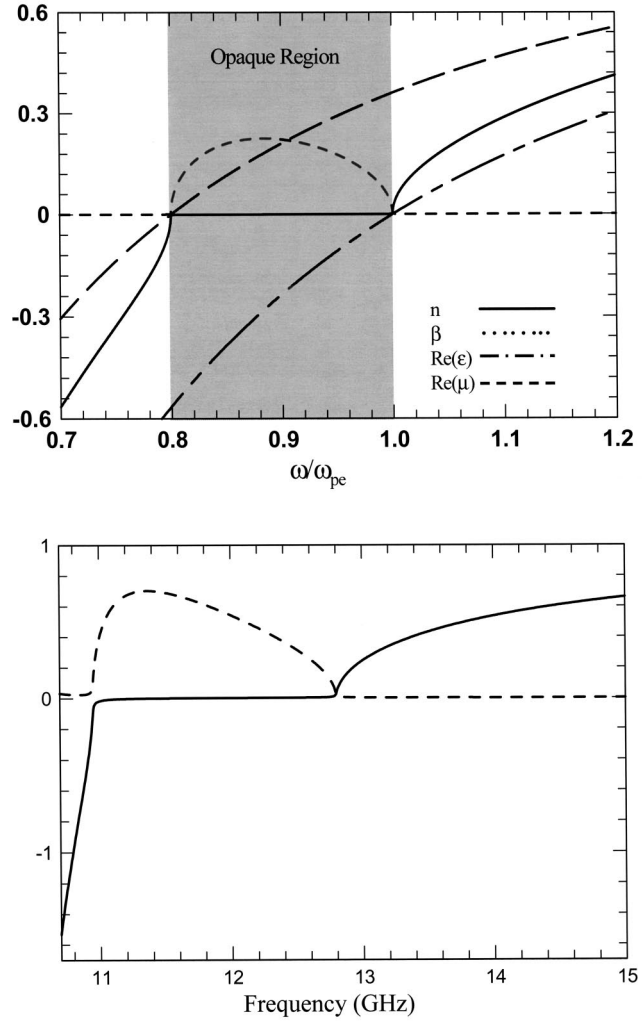

FIG. 1. (a) Refractive index n (thick solid line), extinction coefficient β (short dashed line), $\mathrm{Re}(\varepsilon)$ (long-short dashed line), and $\mathrm{Re}(\mu)$ (dashed line) vs ω/ω_{pe} where ω_{pe} is the electric plasma frequency. In this case we have chosen, in Eq. (3), $\omega_{pm}/\omega_{pe}=0.8$ and $\tilde{\gamma}_e\approx\tilde{\gamma}_m\approx10^{-4}$. In the region where $\mathrm{Re}(\varepsilon)$ and $\mathrm{Re}(\mu)$ have opposite signs the NIM becomes opaque. (b) Refractive index (thick solid line) and extinction coefficient (short dashed line) as calculated from the experimental data reported in Ref. [3]. Note that the parameters in (a) have not been chosen in order to numerically fit the results presented in (b). The comparison only intends to show that the salient characteristics of the refractive index and the extinction coefficient around the opaque region can be qualitatively described by a Drude model.

Before going any further into the details of our analysis we would like to say a few words on the question of how

realistic the lossy Drude model that we use is in describing NIMs. I.e., are there any materials whose properties are described by our Eq. (3)? In order to answer this question we direct the reader's attention to Fig. 1(b), where we show the refractive index and the extinction coefficient in the range between 10.7 and 15 GHz, deduced from the *experimental* data reported in Ref. [3], where the first NIM prototype was experimentally tested and negative refraction demonstrated. The figure shows that the complex refractive index becomes almost a pure imaginary number in the range between 11 and 12.8 GHz, where $-10^{-2} < n < 10^{-2}$. Although the parameters in Fig. 1(a) were not chosen with the intent to fit the experimental data of Fig. 1(b), nevertheless their behavior is remarkably similar in both cases. In other words, the salient characteristics of the refractive index and the extinction coefficient of currently available negative-index metamaterials appear to be well described, around the opaque region, by an effective Drude model, as in our Eq. (3). This is the main reason why the Drude model is widely used in most theoretical efforts [21] that address negative-index materials. The opaque region described in Fig. 1(a) represents an intrinsic gap for the electromagnetic radiation different in nature from the gap formed in photonic band gap (PBG) structures, but with similar pictorial characteristics. In PBG structures the formation of the gap is due to destructive interference caused by the periodic arrangement of scattering or diffracting elements whose sizes are on the order of the incident wavelength. In contrast, NIMs are structured on a much finer scale that ranges from 1/10th to 1/1000th of the wavelength [18], and therefore they respond with an effective dispersion that is essentially due to the bulk properties of the medium. However, while the nature of the gap is different in the two cases, it would be interesting to explore the possibility of using NIMs in the spectral region of opacity as the cladding of a waveguide (see Fig. 2). We begin by first focusing on the TE modes. In this case the electric field is polarized along the y axis (see Fig. 2) and the Helmholtz equation for our geometry is

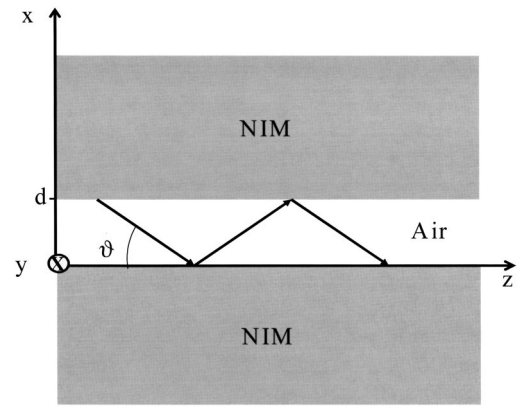

FIG. 2. Schematic representation of the geometry we study. A core of air of thickness d is sandwiched between two identical semi-infinite layers of NIM. ϑ is the angle formed by the wavevector of the radiation with the propagation axis z. The y axis is orthogonal to the plane (x,z).

$$\frac{\partial^2 E_y(x,z)}{\partial x^2} + \frac{\partial^2 E_y(x,z)}{\partial z^2} + \frac{\omega^2}{c^2}\hat{f}(x)E_y(x,z) = 0, \tag{4}$$

where $\hat{f}(x)=\hat{n}^2$ for $x>d$ and $x<0$, while $\hat{f}(x)=n_0$ for $d \geqslant x \geqslant 0$. Here $\hat{n}$ is the refractive index of the NIM and n_0 is the refractive index of the core of the waveguide. The solution of Eq. (4) can be written as follows:

$$E_y(x,z) = \begin{cases} A_1 \exp\left[i\frac{\omega}{c}\left(n_0 z \cos\hat{\vartheta} - \hat{n}x\sqrt{1-\frac{n_0^2\cos^2\hat{\vartheta}}{\hat{n}^2}}\right)\right], & x<0, \\ \exp\left(i\frac{\omega}{c}n_0 z\cos\hat{\vartheta}\right)\left[A_2\exp\left(i\frac{\omega}{c}n_0 x\sin\hat{\vartheta}\right) + A_3\exp\left(-i\frac{\omega}{c}n_0 x\sin\hat{\vartheta}\right)\right], & 0\leqslant x\leqslant d, \\ C\exp\left[i\frac{\omega}{c}\left(n_0 z\cos\hat{\vartheta} + \hat{n}(x-d)\sqrt{1-\frac{n_0^2\cos^2\hat{\vartheta}}{\hat{n}^2}}\right)\right], & x>d, \end{cases} \tag{5}$$

where C is an arbitrary normalization constant that is chosen consistent with the following normalization condition: $\int_{-\infty}^{+\infty}|E_y(x,z=0)|^2\,dx=1$. The choice of the complex parameters A_1, A_2, A_3, and $\hat{\vartheta}$ is determined by imposing that E_y, as well as $(1/\mu)(\partial E_y/\partial x)$, must be continuous at both $x=0$ and $x=d$. The continuity requirements lead to the modal equation for $\hat{\vartheta}$,

$$\tan\left(\frac{\omega}{c}n_0 d\sin\hat{\vartheta}\right) = -i\frac{\frac{2n_0\hat{n}\sin\hat{\vartheta}}{\mu}\sqrt{1-\frac{n_0^2}{\hat{n}^2}\cos^2\hat{\vartheta}}}{n_0^2\sin^2\hat{\vartheta} + \frac{\hat{n}^2}{\mu^2} - \frac{n_0^2}{\mu^2}\cos^2\hat{\vartheta}}, \tag{6}$$

and to the system of linear algebraic equations for A_1, A_2, and A_3:

$$\begin{pmatrix} 1 & -1 & -1 \\ \frac{\hat{n}}{\mu}\sqrt{1-\frac{n_0^2}{\hat{n}^2}\cos^2\hat{\vartheta}} & n_0\sin\hat{\vartheta} & -n_0\sin\hat{\vartheta} \\ 0 & \exp\left(i\frac{\omega}{c}n_0 d\sin\hat{\vartheta}\right) & \exp\left(-i\frac{\omega}{c}n_0 d\sin\hat{\vartheta}\right) \end{pmatrix}\begin{pmatrix} A_1 \\ A_2 \\ A_3 \end{pmatrix} = \begin{pmatrix} 0 \\ 0 \\ C \end{pmatrix}. \tag{7}$$

We note that ϑ (i.e., the angle that the wave vector of the radiation forms with the propagation axis z—see Fig. 2) and the attenuation length L' (i.e., the length along z covered by the radiation before its intensity drops of a factor $1/e$) are linked to the complex parameter $\hat{\vartheta}$ through the following relations:

$$\vartheta = \arccos[\mathrm{Re}(\cos\hat{\vartheta})], \tag{8a}$$

$$L' = \frac{c}{2\omega n_0\,\mathrm{Im}(\cos\hat{\vartheta})}. \tag{8b}$$

The calculation for TM modes follows a development similar to that of TE modes. In the case of TM modes we must impose the continuity conditions on the magnetic field H_y and on $(1/\varepsilon)(\partial H_y/\partial x)$. The solution for TM modes and the modal condition can be obtained from those calculated for TE modes by making the following formal transformations: $E_y \to H_y$ and $\mu \to \varepsilon$.

III. RESULTS AND DISCUSSION

In order to calculate the modes admitted by our waveguide, we have to solve Eq. (6) for TE modes and the corresponding equation for TM modes. Equation (6) is a complex, transcendental equation that does not admit analytical solutions. It can be solved numerically by using the Newton-Rapson method [22]. Then, by using Eqs. (5) and (7), we can calculate the transverse-mode profile for different propagation distances. In Fig. 3 we show TE-guided modes for a

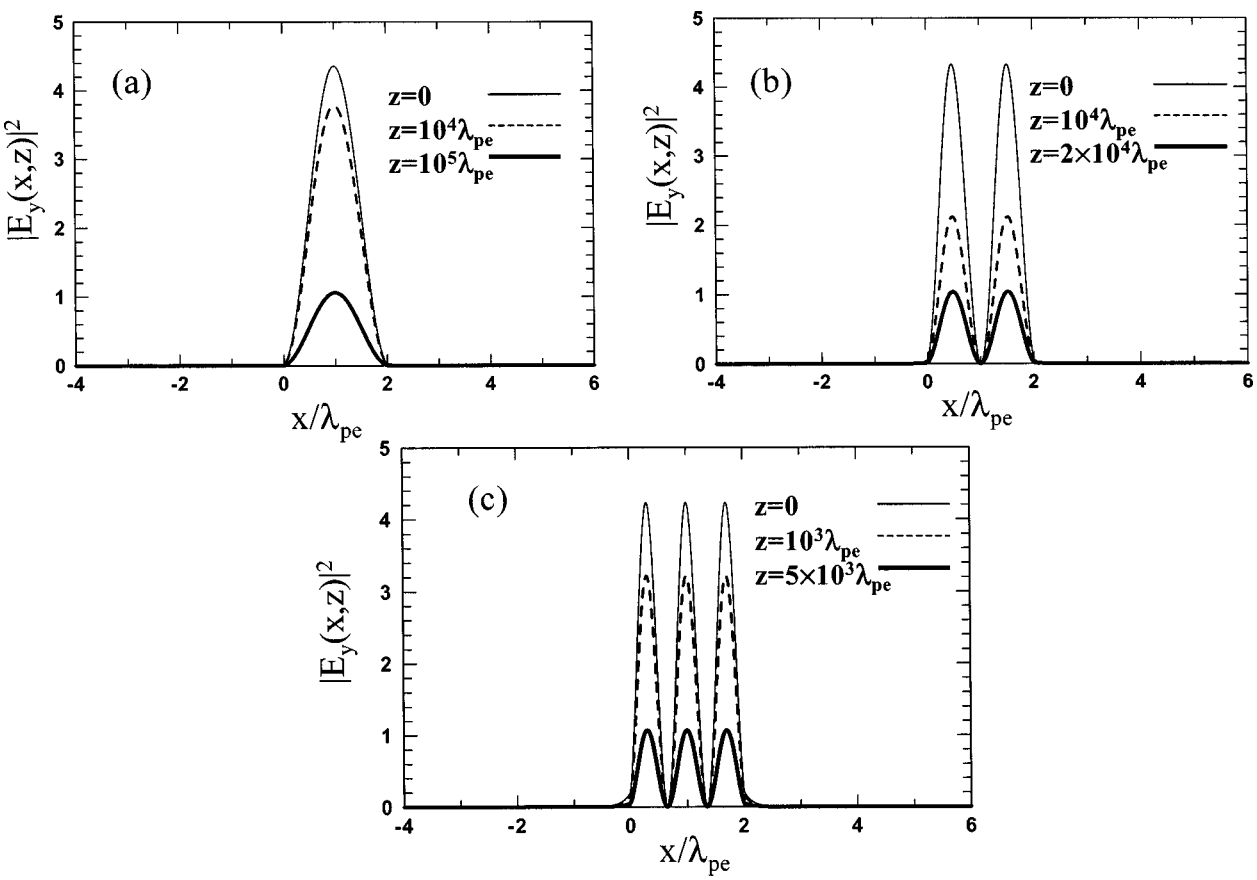

FIG. 3. Transverse profile of the TE guided modes at different propagation distances for a waveguide whose air core has a thickness $d=2\lambda_{pe}$, $\lambda_{pe}=2\pi c/\omega_{pe}$. The frequency of the field is $\omega=0.88\omega_{pe}$. (a) TE_0, (b) TE_1, and (c) TE_2. The electric field is expressed in normalized units according to the normalization condition $\int_{-\infty}^{+\infty}|E_y(x,z=0)|^2dx=1$.

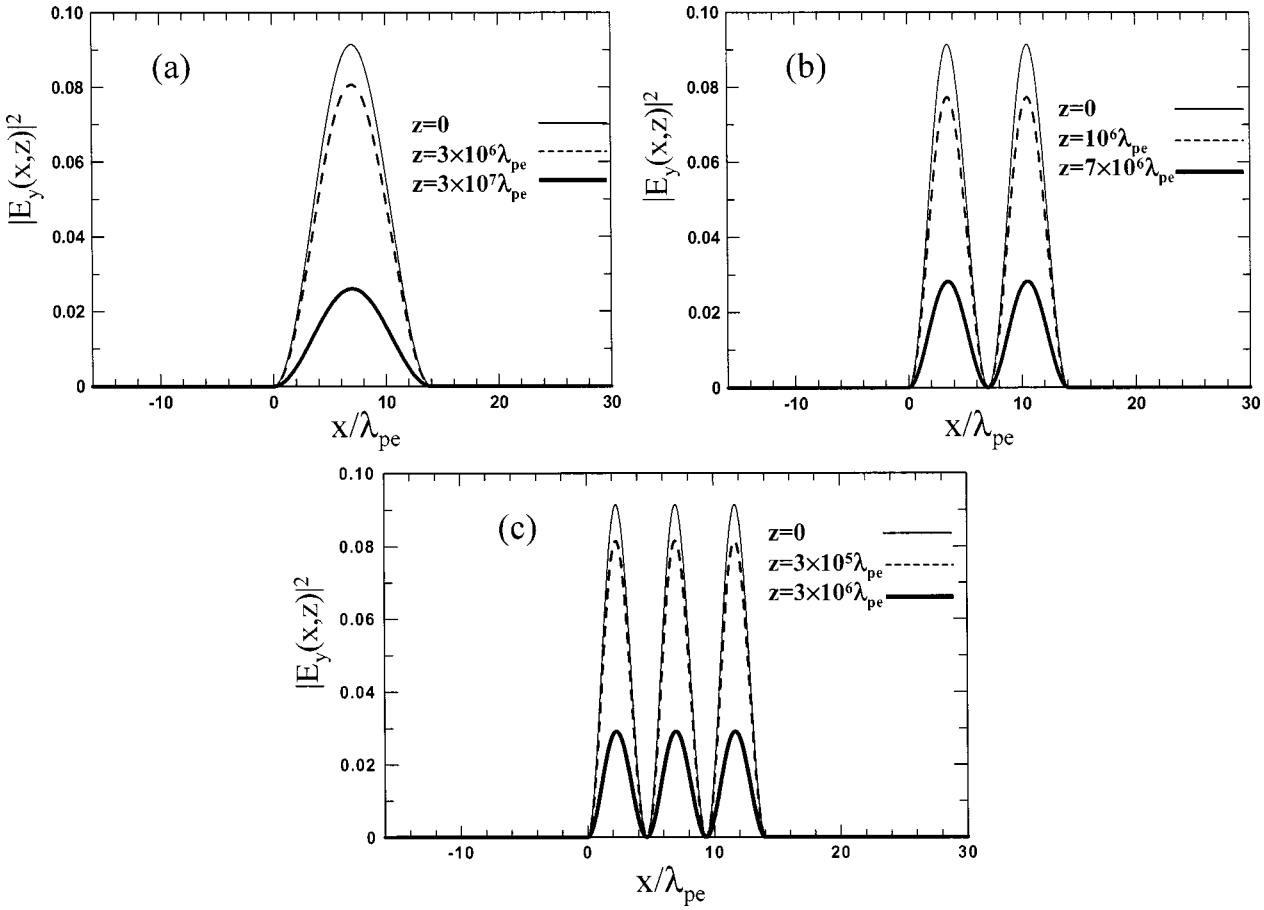

FIG. 4. Transverse profile of the first three TE guided modes at different propagation distances for a waveguide whose air core has a thickness $d=14\lambda_{pe}$. (a) TE_0, (b) TE_1, and (c) TE_2. The electric field is expressed in normalized units according to the normalization condition $\int_{-\infty}^{+\infty}|E_y(x,z=0)|^2dx=1$.

waveguide whose core has thickness $d=2\lambda_{pe}$, where $\lambda_{pe}=2\pi c/\omega_{pe}$. The dispersion properties of the NIM are those described in Fig. 1. The electromagnetic field is approximately tuned at the center of the opaque region of the NIM, where $\omega=0.88\omega_{pe}$. The thickness of the core is in this case large enough to accommodate three confined modes at different angles: $\vartheta\cong 15.9°$ for TE_0, $\vartheta\cong 33°$ for TE_1, and $\vartheta\cong 53.9°$ for TE_2. In the case of the fundamental mode (TE_0), we find an attenuation length of approximately $L'\cong 7\times 10^4\lambda_{pe}$. Supposing that that the waveguide operates around 10 μm, the attenuation length is approximately 0.7 m, which corresponds to a loss factor of approximately 6 dB/m. The losses drastically drop for larger core diameters, as shown in Fig. 4, where the core is $d=14\lambda_{pe}$. In the case of Fig. 4, for an operational wavelength around 10 μm, the attenuation length of the TE_0 mode is approximately 240 m, the losses are approximately 0.01 dB/m and the size of the air core is only 140 μm. In this case the guide accommodates a large number of modes at different angles. The first three modes are excited respectively at $\vartheta\cong 2.2°$, $\vartheta\cong 4.4°$, and $\vartheta\cong 6.6°$. In Fig. 5 we show the TM_0 mode for (a) $d=2\lambda_{pe}$ and (b) $d=14\lambda_{pe}$. In the case of Fig. 5(a) the angle formed by the wave vector with the z axis is $\vartheta\cong 17.3°$ and the attenuation length is $L'\cong 3.4\times 10^4\lambda_{pe}$, which corresponds to approximately 12 dB/m in losses for a wavelength of 10 μm. In Fig. 5(b), $\vartheta\cong 2.3°$, $L'\cong 1.4\times 10^7\lambda_{pe}$, and the losses are of the order of 0.03 dB/m. Note that in the case we have studied the TE guided modes have longer attenuation lengths than the TM guided modes, and in the opaque region of the NIM, $\mathrm{Re}(\varepsilon)$ is less than zero, while $\mathrm{Re}(\mu)$ is greater than zero. If we consider the opposite case—i.e., $\mathrm{Re}(\varepsilon)>0$ and $\mathrm{Re}(\mu)<0$—the TM guided modes would have a longer attenuation length than the TE guided modes.

Finally we note that recently waveguides with an air core and a cladding made by a two-dimensional square array of silver nanowires embedded in an air host medium have been numerically demonstrated to guide at optical frequency more efficiently than silver waveguides [23]: the effective extinction coefficient of the nanostructured cladding is smaller than that of a homogeneous silver cladding. In the case of Ref. [23] the effective index of the cladding can be made to vary in the range $0<n<1$, depending on the ratio between the width of the silver wires and the periodicity of the array. Of course, a metamaterial designed in this way is by definition not a NIM and light refraction will be right handed as in standard positive index materials. In this work we have instead explored the guiding properties of a NIM in its opaque region—i.e., in the region where its refractive index varies in the range $-10^{-2}<n<10^{-2}$.

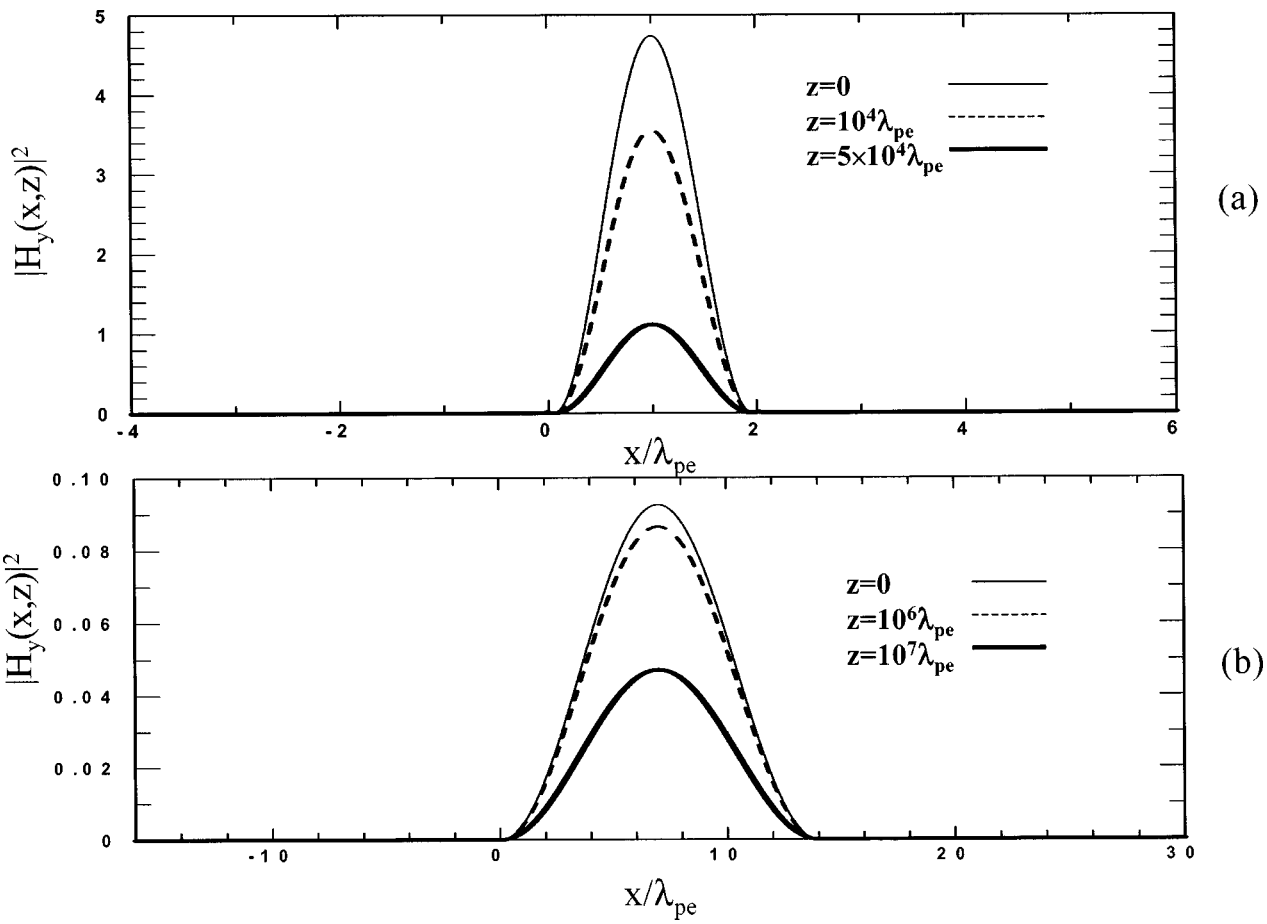

FIG. 5. Transverse profile of the TM_0 mode for different propagation distances. The waveguide has an air core of thickness, respectively, (a) $d=2\lambda_{pe}$ and (b) $d=14\lambda_{pe}$. The magnetic field is expressed in normalized units according to the normalization condition $\int_{-\infty}^{+\infty}|H_y(x,z=0)|^2dx=1$.

IV. CONCLUSIONS

In conclusion, we have studied a symmetric hollow waveguide made with a NIM cladding. In the opacity region of the NIM, the waveguide admits both TE and TM guided modes with relatively low losses. While further material development is still needed, recent advancements in the design of metamaterials suggest that this waveguide could operate in the infrared regime with better performances compared to more traditional hollow waveguides.

ACKNOWLEDGMENT

G.D' Aguanno wishes to thank A.M. Zheltikov for helpful discussions.

[1] V. G. Veselago, Sov. Phys. Usp. **10**, 509 (1968).
[2] J. B. Pendry, Phys. Rev. Lett. **85**, 3966 (2000).
[3] R. A. Shelby, D. R. Smith, and S. Schultz, Science **292**, 77 (2001).
[4] Focus issue on Negative Refraction and Metamaterials, Opt. Express **11**, 639 (2003) and references therein.
[5] A. Yariv and P. Yeh, *Optical Waves in Crystals* (Wiley, New York, 1984).
[6] P. W. Smith, Appl. Phys. Lett. **19**, 132 (1971).
[7] T. J. Bridges, E. G. Burkhardt, and P. W. Smith, Appl. Phys. Lett. **20**, 403 (1972).
[8] P. K. Tien, R. J. Martin, and S. Riva-Sanseverino, Appl. Phys. Lett. **27**, 251 (1975).
[9] E. A. J. Marcatili and R. A. Schmeltzer, Bell Syst. Tech. J. **43**, 1783 (1964).
[10] J. A. Harrington and C. C. Gregory, Opt. Lett. **15**, 541 (1990).
[11] J. Dai and J. A. Harrington, Appl. Opt. **36**, 5072 (1997).
[12] Y. Matsuura and M. Miyagi, Appl. Opt. **32**, 6598 (1993).
[13] J. C. Knight *et al.*, Science **282**, 1476 (1998).
[14] R. F. Cregan *et al.*, Science **285**, 1537 (1999).
[15] I. V. Shadrivov, A. A. Sukhorukov, and Y. S. Kivshar, Phys. Rev. E **67**, 057602 (2003); Bae-Ian Wu *et al.*, J. Appl. Phys. **93**, 9386 (2003).
[16] S. O' Brien and J. B. Pendry, J. Phys.: Condens. Matter **14**,

6393 (2002).

[17] S. O' Brien *et al.*, Phys. Rev. B **69**, 241101(R) (2004), and references therein.

[18] J. Pendry, Opt. Photonics News **15**(9), 33 (2004).

[19] L. D. Landau and E. M. Lifshitz, *Electrodynamics of Continuous Media* (Pergamon, New York, 1960).

[20] Note that while solving Eq. (1) with the condition $\beta > 0$ leads to the correct expressions of the refractive index and the extinction coefficient as given in Eqs. (2). On the other hand, solving Eq. (1) with the condition $n > 0$ leads to the following expressions:

$$n = \frac{\sqrt{\mathrm{Re}(\varepsilon\mu) + \sqrt{[\mathrm{Re}(\varepsilon\mu)]^2 + [\mathrm{Im}(\varepsilon\mu)]^2}}}{\sqrt{2}},$$

$$\beta = \frac{\mathrm{Im}(\varepsilon\mu)}{\sqrt{2}\sqrt{\mathrm{Re}(\varepsilon\mu) + \sqrt{[\mathrm{Re}(\varepsilon\mu)]^2 + [\mathrm{Im}(\varepsilon\mu)]^2}}}.$$

The above expressions are equivalent to those given into Eqs. (2) only when $\mathrm{Im}(\varepsilon\mu) > 0$ and they cannot be considered valid in general.

[21] In addition to Pendry's work cited in Ref. [2] we give here a list of other theoretical papers where the dispersive properties of a NIM are described through a Drude model as in our Eq. (3): W. Ziolkowski and E. Heyman, Phys. Rev. E **64**, 056625 (2001); R. W. Ziolkowski and A. D. Kipple, *ibid.* **68**, 026615 (2003); R. W. Ziolkowski, Opt. Express **11**, 662 (2003); Phys. Rev. E **70**, 046608 (2004); G. D' Aguanno *et al.*, Phys. Rev. Lett. **93**, 213902 (2004). In addition to Ref. [3]—that is, the case explicitly considered for the comparison drawn in Fig. 1—several other experimental papers have been published where a NIM material has been realized with dispersive properties that can be described in a particular spectral range by a Drude model as in our Eq. (3). We cite, for example, D. R. Smith *et al.*, Phys. Rev. Lett. **84**, 4184 (2000); C. G. Parazzoli *et al.*, *ibid.* **90**, 107401 (2003); S. Linden *et al.*, Science **306**, 1351 (2004). In the last paper a magnetic resonance has been implemented at 100 THz.

[22] W. H. Press, B. P. Flannery, S. A. Teukolsky, and W. T. Vetterling, *Numerical Recipes in C* (Cambridge University Press, Cambridge, England, 1988). In our case the Newton-Rapson procedure is initialized with a trial solution $\hat{\vartheta}_0$, which solves the following equation:

$$\tan\left(\frac{\omega}{c} n_0 d \sin\hat{\vartheta}_0\right) = \mathrm{Re}\left[-i\frac{\dfrac{2n_0\hat{n}\sin\hat{\vartheta}_0}{\mu}\sqrt{1-\dfrac{n_0^2}{\hat{n}^2}\cos^2\hat{\vartheta}_0}}{n_0^2\sin^2\hat{\vartheta}_0 + \dfrac{\hat{n}^2}{\mu^2} - \dfrac{n_0^2}{\mu^2}\cos^2\hat{\vartheta}_0}\right].$$

[23] B. T. Schwartz and R. Piestun, Appl. Phys. Lett. **85**, 1 (2004).